# LUMINOUS TRANSMITTANCE AND PHASE TRANSITION TEMPERATURE OF VO$_2$:CE THIN FILMS PREPARED BY DC REACTIVE MAGNETRON SPUTTERING

**Ambonisye S[a], Samiji ME[b] and Mlyuka NR[b]**

[a]*Physics Unit, Faculty of Science, Dar es Salaam University College of Education, P.O. Box 2329, Dar es Salaam, Tanzania; E-mail: ambogib2005@yahoo.com*
[b]*Department of Physics, College of Natural and Applied Sciences, University of Dar es Salaam, Tanzania; E-mail: esamiji@gmail.com*

**ABSTRACT**

*Vanadium dioxide (VO$_2$) and cerium-doped vanadium dioxide (VO$_2$:Ce) thin films were prepared by DC reactive magnetron sputtering from vanadium metallic target and V-Ce alloy targets. Luminous transmittance and phase transition temperatures of the films were studied. The Shimadzu SOLIDSPEC-3700 DUV-VIS-NIR spectrophotometer was used to measure the transmittance and reflectance of the films. The phase transition temperature ($\tau_c$) of the films was obtained from both the transmittance and sheet resistance against temperature curves. A change in sheet resistance of 2 to 3 orders of magnitude was observed for both undoped and Ce-doped VO$_2$ films. Comparison between undoped and doped VO$_2$ films revealed that cerium inclusion altered both the visible and infrared transmittance of VO$_2$ thin films. Luminous transmittance was slightly enhanced while $\tau_c$ was slightly depressed by cerium inclusion in VO$_2$. A two-step increase in transmittance observed in the cooling loop in pure VO$_2$ was found to be suppressed by cerium inclusion.*

**Keywords**: *vanadium dioxide, luminous transmittance, phase transition temperature*

## INTRODUCTION

Discovery of novel behavior of vanadium dioxide to undergo a metal-to-insulator phase transition at a temperature ($\tau_c$) of ~68 $^o$C accompanied by dramatic changes in electrical and optical properties has attracted intensive research in this thermochromic material. The phase transition in VO$_2$ has been tailored to suit various applications in devices such as smart windows, thermal sensors and switching devices (Miyazaki and Yasui 2006). However, the transition temperature is too high for smart window applications and it is therefore desirable for it to be reduced. Many studies have been conducted to lower $\tau_c$ to the vicinity of room temperature especially through doping with foreign atoms such as tungsten,

molybdenum, niobium and fluorine. Although tungsten (W) doping has shown incredible reduction in $\tau_c$ to room temperature (Batista *et al.* 2011), W-doped VO$_2$ films are reported to have lower infrared transmittance at room temperature compared with the undoped films (Wang *et al.* 2005), and hence unsuitable for high performance optical switching applications.

Several techniques have been reported for depositing VO$_2$-based thin films including, sputtering (Kivaisi and Samiji 1999), reactive evaporation (Golan *et al.* 2004), chemical vapor deposition (CVD) (Manning *et al.* 2005), pulsed laser deposition (PLD) (Lappalainen *et al.* 2009), molecular beam epitaxy (MBE) (Rata

*et al.* 2003) and sol-gel process (Lu *et al.* 1999). Despite requirement of expensive equipment, sputtering offers several advantages such as the ability to produce uniform films and efficient deposition (Kiri *et al.* 2010). It is also one of the most promising techniques for large-area and large-scale coating applications (Sobhan *et al.* 1996). This paper reports the luminous transmittance and $\tau_c$ of Ce-doped $VO_2$ ($VO_2$:Ce) thin films.

**MATERIALS AND METHODS**

$VO_2$ and $VO_2$:Ce thin films were prepared by reactive DC magnetron sputtering of metallic V target and V-Ce alloy targets (99.9 % purity) using the BALZERS BAE 250 coating unit. This preparation technique was also employed by Kivaisi and Samiji 1994. Both $VO_2$ and $VO_2$:Ce thin films were deposited on normal microscope quartz glass substrates placed ~16 cm above the target. The alloy targets had varying percentage compositions of vanadium and cerium as V99 %-Ce1 %, V98 %-Ce2 % and V96 %-Ce4 %. Prior to the deposition, the vacuum chamber was evacuated down to a base pressure of ~3.0 x$10^{-5}$ mbar. The sputtering gas, Ar (99.999 % purity) and reactive gas, $O_2$ (99.999 % purity) were introduced in the chamber at the flow rates of 75 and 4.4 to 4.7 ml$_n$/min, respectively. The working pressure was maintained at about 3.8 x$10^{-3}$ mbar and the sputtering power was 200 watts. The substrate temperature at which the films were deposited was ~420 $^o$C. Deposition rates were about 3.6 nm/min and 3.4 nm/min for $VO_2$ and $VO_2$:Ce films, respectively.

Electrical measurements were performed using a two-point probe and the JANDEL MODEL RM3-AR test unit which works in combination with the four-point probe. In order to determine temperature dependence of sheet resistance the films were placed on a temperature regulated hotplate whose temperature was varied within the interval $25 < T_e < 100$ $^o$C. The heating and cooling rates were ~10 $^o$C/min and ~0.5 $^o$C/min, respectively near 25 $^o$C, and ~7 $^o$C/min and ~5 $^o$C/min, respectively near 100 $^o$C. For optical characterization, the Shimadzu SOLIDSPEC-3700 DUV-VIS-NIR spectrophotometer was used. A heating cell was used to change the film surface temperature between ~25 $^o$C and ~100 $^o$C when measuring the transmittance of the films as a function of temperature. The rate of heating was ~10 $^o$C/min near room temperature and ~6 $^o$C/min near 100 $^o$C while the cooling rate was ~5 $^o$C/min near 100 $^o$C and ~0.8 $^o$C/min near 25 $^o$C. Integrated luminous (lum) and solar (sol) transmittance values were obtained from the equation,

$$T_{lum(sol)}(\theta) = \frac{\int_a^b \psi_{lum(sol)}(\theta,\lambda)T(\theta,\lambda)d\lambda}{\int_a^b \psi_{lum(sol)}(\theta,\lambda)d\lambda} \quad ......(1)$$

where the integral is evaluated from $a = 0.38$ to $b = 0.76$ μm for luminous transmittance and from $a = 0.25$ to $b = 2.5$ μm for solar transmittance, $\psi_{lum}$ is the spectral sensitivity of the light-adapted human eye, and $\psi_{sol}$ is the solar irradiance spectrum ASTM G-173 for air mass 1.5 (corresponding to the sun standing 37$^o$ above the horizon).

**RESULTS AND DISCUSSION**

  *a) Electrical Properties of VO$_2$ and VO$_2$:Ce Thin Films*

Both $VO_2$ and $VO_2$:Ce thin films exhibited sheet resistance change of about three orders of magnitude across the phase transition. This is a typical behavior for $VO_2$ films deposited on amorphous substrates (Béteille *et al.* 1997). The variation of sheet resistance with temperature for undoped and cerium-doped $VO_2$ thin films measured using a two-point probe are shown in Figure 1. A two-step decrease in sheet resistance (i.e. with two points of inflexion) was observed in the heating loop for all the films, an observation that was also reported by

Kivaisi and Samiji 1999. The sheet resistance determined by the JANDEL four point probe however, did not register the step. The drop in sheet resistance exhibited by all the films was
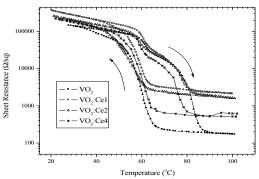


**Figure 1:** Variation of sheet resistance with temperature for $VO_2$, $VO_2$:Ce1, VO2:Ce2 and VO2:Ce4 thin films (~100 nm thick, deposited at 420 °C) measured using a two-point probe.

not very sharp (Figure 1). This could be caused by the presence of large number of microscopic crystals each characterized by its own $\tau_c$ and hysteresis loop, whose totality blurred and broadened the switching. The figure also shows a decrease in both the transition temperature and the hysteresis loop width with increasing cerium concentration. The loop widths were 20.31 °C, 13.43 °C, 16.68 °C and 12.96 °C for $VO_2$, $VO_2$:Ce1, $VO_2$:Ce2 and $VO_2$:Ce4 thin films, respectively. Jin and Tanemura 1995 attributed such a change in hysteresis loop width to improvement of crystallinity and microstructure. It also appeared that increase in Ce content made the high temperature phase of $VO_2$ less conducting. Similar behavior was observed by Béteille *et al.* 1997 for titanium-doped $VO_2$ thin films. For $VO_2$, $VO_2$:Ce1 and $VO_2$:Ce2 films, the temperatures at which the phase change occurred took a decreasing order. However, it appeared to go up again for $VO_2$:Ce4 film.

## b) Optical Properties of $VO_2$ and $VO_2$:Ce Thin Films
### (i) Luminous Transmittance
The inclusion of cerium in $VO_2$ influenced changes in luminous transmittance of $VO_2$ films. The low temperature phase of undoped $VO_2$ had a maximum transmittance of about 34 % at ~710 nm while it was ~40.6 % at ~651 nm for $VO_2$:Ce1, ~35.6 % at ~650 nm for $VO_2$:Ce2 and ~38.7 % at ~638 nm for $VO_2$:Ce4. Small transmittance values for the films in the visible region were considered to originate from the strong intra-band and inter-band absorption in the short-wavelength range for both the metallic and semiconductive phases as cited by Zhang *et al.* 2010. The increase in luminous transmittance for Ce-doped $VO_2$ was thought to be attributed to replacement of $V^{4+}$ by $Ce^{3+}$ which resulted into oxygen vacancies. The
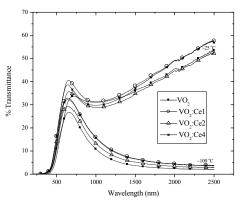


**Figure 2**: Spectral transmittance for single $VO_2$, $VO_2$:Ce1, $VO_2$:Ce2 and $VO_2$:Ce4 thin films (~100 nm thick, deposited at 420 °C).

observed slight shift of the maximum transmittance in the visible region to lower wavelengths justified the small change in color of the films. There was a significant modulation in visible transmittance for low and high temperature phases for both undoped and Ce-doped $VO_2$ thin films owing to free career concentration differences. The high temperature

phase of undoped VO₂ had a maximum transmittance of about 26.5 % at 663 nm while it was ~33 % at 643 nm for VO₂:Ce1, ~29.3 % at 642 nm for VO₂:Ce2 and ~34 % at 650 nm for VO₂:Ce4 (Figure 2).

Integrated luminous transmittance ($T_{lum}$) values (at ~25 °C) computed using Equation 1 revealed a $T_{lum}$ of 18.9 %, 27.9 %, 23.9 % and
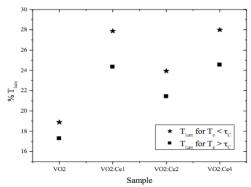


**Figure 3**: Integrated luminous transmittance ($T_{lum}$) for VO₂, VO₂:Ce1, VO₂:Ce2 and VO₂:Ce4 thin films (~100 nm thick, deposited at 420 °C)
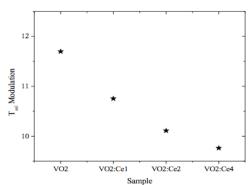


**Figure 4**: Integrated solar transmittance ($T_{sol}$) modulation for VO₂, VO₂:Ce1, VO₂:Ce2 and VO₂:Ce4 thin films (~100 nm thick, deposited at 420 °C).

28 % for VO₂, VO₂:Ce1, VO₂:Ce2 and VO₂:Ce4, respectively. For the high temperature phase (at ~100 °C), the $T_{lum}$ values

were 17.3 %, 24.3 %, 21.4 % and 24.5 % for VO₂, VO₂:Ce1, VO₂:Ce2 and VO₂:Ce4, respectively. The differences in $T_{lum}$ values for the low- and high-temperature phases of VO₂ compare with the results reported by Xu *et al.* 2004 for 50 nm VO₂ films on quartz glass. The $T_{lum}$ values are shown in Table 1 and the general trend is represented in Figure 3. It could generally be suggested from Figure 3 that the inclusion of cerium increased the visible transmittance of VO₂ thin films.

***(ii) Solar and Infrared Transmittance***
Integrated solar transmittance ($T_{sol}$) values at ~25 °C were 26.5 %, 29.2 %, 26.7 % and 27.9 % for VO₂, VO₂:Ce1, VO₂:Ce2 and VO₂:Ce4 thin films, respectively. Comparatively, Khan and Granqvist 1989 obtained a $T_{sol}$=31 % for a 75 nm thick VO₂ thin film at 25 °C. In this study, $T_{sol}$ values at ~100 °C were 13.7 %, 18.6 %, 16.2 % and 18.5 % for VO₂, VO₂:Ce1, VO₂:Ce2 and VO₂:Ce4 thin films, respectively. $T_{sol}$ modulation shown in Figure 4 indicates that inclusion of cerium in VO₂ slightly decreased its solar modulation.

The near infrared (NIR) transmittance data extracted from Figure 2 give transmittance contrasts of 51.4 % for VO₂, 54.3 % for VO₂:Ce1, 49.5 % for VO₂:Ce2 and 53.3 % for VO₂:Ce4 all at λ = 2500 nm. From Figure 2, VO₂:Ce1 is observed to be the most transmitting at 2500 nm and has the highest NIR transmittance contrast for all Ce concentration values studied. These data are supported by the transmittance-versus-temperature curves at a wavelength of about 2500 nm shown in Figure 5. The infrared transmittance of the films dropped drastically to values below 3 %, an indication that the reflectivities of these films at 2500 nm were quite high as reported by Béteille *et al.* 1997. The transmittance hysteresis loop widths for VO₂ films appeared to decrease with increase in
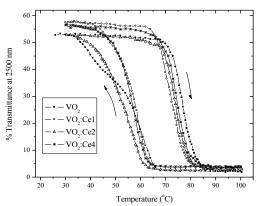
**Figure 5**: NIR switching and hysteresis loops in $VO_2$ and $VO_2$:Ce thin films (~100 nm thick, deposited at 420 $^o$C) obtained using the Shimadzu SOLIDSPEC-3700 DUV-VIS-NIR spectrophotometer.
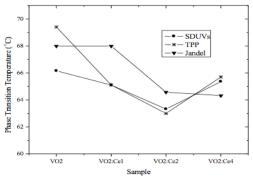


**Figure 6**: Transition temperature for $VO_2$ and $VO_2$:Ce thin films obtained from transmittance-vs-temperature and sheet resistance-vs-temperature curves. SDUVs = Shimadzu SOLIDSPEC-3700 DUV-VIS-NIR spectrophotometer, TPP = two-point probe, Jandel = JANDEL four-point probe unit.

cerium concentration. A two-step increase in transmittance was observed in the cooling loop in pure $VO_2$. This could be due to the formation of an intermediate metastable phase called $M_2$, between the usual monoclinic ($M_1$) and rutile (R) phases (Béteille and Livage 1998). However, the two-step increase in transmittance appeared to be suppressed by cerium inclusion.

### c) Effect of Cerium Doping on Phase Transition Temperature of $VO_2$ Thin Films

From the sheet resistance versus temperature curves for $VO_2$ and $VO_2$:Ce samples, it was noted that dramatic changes in sheet resistance for $VO_2$ occurred at a phase transition temperature, $\tau_c \sim 69$ $^o$C. This value is close to that of the bulk $VO_2$ ($\tau_c \sim 68$ $^o$C). The transition temperatures for $VO_2$:Ce films were about 65 $^o$C, 63 $^o$C and 66 $^o$C for $VO_2$:Ce1, $VO_2$:Ce2 and $VO_2$:Ce4 thin films, respectively. The $VO_2$:Ce thin films had the $\tau_c$ slightly lower than that of undoped $VO_2$ thin films (Figure 6). The reduction in $\tau_c$ can be due to thermal expansion miss-match, intrinsic stress, presence of second phase (deviation from stoichiometry) or addition of impurities (doping). It was suggested in this case that inclusion of cerium induced a change in the V-O and V-V distances of the $VO_2$ structure due to the differences in ionic radii between $Ce^{3+}$ (0.102 nm) and $V^{4+}$ (0.059 nm). This caused phase transitions at lower temperatures than that for undoped $VO_2$ thin films as it was reported by Lu *et al.* 1996. This conforms to the findings by Kiri *et al.* 2010 who reported that dopants with atomic radii larger than the $V^{4+}$ ion cause a decrease in $\tau_c$ whereas those with smaller ionic radii increase $\tau_c$. Table 1 summarises major properties of $VO_2$ and $VO_2$:Ce thin films.

### CONCLUSIONS

$VO_2$ and cerium-doped $VO_2$ thin films have been successfully prepared by reactive DC magnetron sputtering. The films had sheet resistance switching by 2 to 3 orders of magnitude. The maximum transmittances in the visible region, ranging from 34-40 % and 26-34 % were observed for $\tau < \tau_c$ and $\tau > \tau_c$

5

**Table 1**: Summary of the properties of undoped and Ce-doped $VO_2$ thin films

| Property | Sample | | | |
|---|---|---|---|---|
| | $VO_2$ | $VO_2$:Ce1 | $VO_2$:Ce2 | $VO_2$:Ce4 |
| Max % $T_L$ ($\lambda$) | 34 (710) | 40.6 (651) | 35.6 (650) | 38.7 (638) |
| Max % $T_H$ ($\lambda$) | 26.9 (656.5) | 29.3 (639.5) | 32.2 (638) | 32.9 (645) |
| % T at 555 nm (H, L) | 17.9, 18.52 | 26.1, 28.27 | 22.8, 24.16 | 26.3, 28.88 |
| $T_{lum}$ at ~25 $^o$C | 18.89 | 27.88 | 23.93 | 28.00 |
| $T_{lum}$ at ~100 $^o$C | 17.28 | 24.33 | 21.42 | 24.54 |
| $T_{sol}$ at ~25 $^o$C | 25.43 | 29.35 | 26.34 | 28.29 |
| $T_{sol}$ at ~100 $^o$C | 13.73 | 18.60 | 16.24 | 18.53 |
| $\tau_c$ (SolidSpec-3700 DUV) | 66.16 | 65.10 | 63.32 | 65.36 |
| $\tau_c$ (TPP) | 69.40 | 65.10 | 63.00 | 65.70 |
| $\tau_c$ (Jandel) | 67.99 | 67.99 | 64.57 | 64.32 |
| Hysteresis Width (TPP) | 20.31 | 13.43 | 16.68 | 12.96 |
| Hysteresis Width (Jandel) | 10.64 | 6.58 | 6.84 | 7.85 |
| Hysteresis Width (SOLIDSPEC-3700DUV) | 21.14 | 14.90 | 20.86 | 18.01 |
| % T Contrast | 51.37 | 54.27 | 49.54 | 53.25 |
| Key: H = High temperature phase, L = Low temperature phase TPP = Two point probe | | | | |

respectively. The integrated luminous transmittance ($T_{lum}$) increased as the result of cerium doping in $VO_2$. The integrated solar transmittance ($T_{sol}$) of the $VO_2$:Ce films increased as cerium concentration increased. The hysteresis loop widths decreased as the result of cerium inclusion in $VO_2$. A two-step increase in transmittance observed in the cooling loop in $VO_2$ was suppressed by cerium doping. On the other hand, cerium doping in $VO_2$ was observed to decrease its phase transition temperature.

**References**
Batista C, Ribeiro RM and Teixeira V 2011. Synthesis and characterization of $VO_2$-based thermochromic thin films for energy-efficient windows. *Nanoscale Research Letters*: 1-7

Béteille F and Livage J 1998. Optical switching in $VO_2$ thin films. *J. Sol-Gel Sc. Tech.* **13**: 915-921

Béteille F, Morineau R, Livage J and Nagano M 1997. Switching properties of $V_{1-x}Ti_xO_2$ thin films deposited from alkoxides. *Materials Research Bulletin* **32**(8): 1109-1117

Golan G, Axelevitch A, Sigalov B and Gorenstein B 2004. Investigation of phase transition mechanism in vanadium oxide thin films. *J. Optoelectronics and Advanced Mater.* **6**(1): 189-195

Jin P and Tanemura S. 1995. Relationship between transition temperature and x in $V_{1-x}Mo_xO_2$ films deposited by dual-target magnetron sputtering. *Jpn. J. Appl. Phys.* **34**: 2459-2460

Khan KA and Granqvist CG 1989. Thermochromic sputter-deposited vanadium oxyfluoride coatings with low luminous absorptance. *Appl. Phys. Lett.* **55**: 4-6

Kiri P, Hyett G and Binions R 2010. Solid state thermochromic materials. *Adv. Mat. Lett.* **1**(2): 86-105

Kivaisi RT and Samiji M 1999. Optical and electrical properties of vanadium dioxide films prepared under optimized rf sputtering conditions. *Solar Energy Materials and Solar Cells* **57**: 141-152

Lappalainen J, Heinilehto S, Jantunen H and Lantto V 2009. Microstructure

dependent switching properties of $VO_2$ thin films. *J. Electroceram* **22**: 73-77

Lu S, Hou L and Gan F 1996. Synthesis and phase transition of $Cu^{2+}$ ion doped $VO_2$ thin films. *Journal of Mater. Science Letters* **15**: 856-857

Lu S, Hou L and Gan F 1999. Surface analysis and phase transition of gel-derived $VO_2$ thin films. *Thin Solid Films* **353**: 40-44

Manning TD, Parkin IP, Blackman C and Qureshi U 2005. APCVD of thermochromic vanadium dioxide thin films: solid solutions $V_{2-x}M_xO_2$ (M = Mo, Nb) or composites $VO_2:SnO_2$. *J. Mater. Chem.* **15**: 4560-4566

Miyazaki H and Yasui I 2006. Substrate bias effect on the fabrication of thermochromic $VO_2$ films by reactive rf sputtering. *J. Phys. D: Appl. Phys.* **39**: 2220-2223

Rata AD, Chezan AR, Presura C and Hibma T 2003. Electrical properties of epitaxially grown $VO_x$ thin films. *Surface Science* **532–535**: 341-345

Sobhan MA, Kivaisi RT, Stjerna B and Granqvist CG 1996. Thermochromism of sputter deposited $W_xV_{1-x}O_2$ films. *Solar Energy Materials & Solar Cells* **44**: 451-455

Wang H, Yi X and Li Y 2005. Fabrication of $VO_2$ films with low transition temperature for optical switching applications. *Optics Communications* **256**: 305-309

Xu G, Jin P, Tazawa M and Yoshimura K 2004. Tailoring of luminous transmittance upon switching for thermochromic $VO_2$ films by thickness control. *Jpn. J. Appl. Phys.* **43**: 186-187

Zhang Z, Gao Y, Chen Z, Du J, Cao C, Kang L and Luo H 2010. Thermochromic $VO_2$ thin films: solution-based processing improved optical properties and lowered phase transformation temperature. *Langmuir* **26**(13): 10738-10744